

## Nitric oxide modulation of the electrically excitable skin of *Xenopus laevis* frog tadpoles

Michael H. Alpert, HongYan Zhang, Micol Molinari, William J. Heitler and Keith T. Sillar\*

*School of Biology, University of St Andrews, St Andrews, Fife, KY16 9TS, UK*

\*Author for correspondence (e-mail: kts1@st-andrews.ac.uk)

Accepted 30 August 2007

### Summary

Nitric oxide (NO) is a highly diffusible signalling molecule with widespread effects on the integrative electrical properties of a variety of neuronal and muscle cells. We have explored the effects of NO on the cardiac-like impulse generated by skin cells of the hatchling *Xenopus* tadpole. Skin cell impulses propagate from cell to cell *via* gap junctions and form an unusual sensory system, which triggers escape behaviour at early stages of amphibian development. We show that the NO donor S-nitroso-*N*-acetylpenicillamine (SNAP) increases the duration of the skin impulse and slows the rate of impulse propagation across the skin, and also produces a significant

depolarization of the membrane potential of skin cells. Each of these effects of SNAP is significantly reversed by the NO scavenger, C-PTIO. Possible sources of NO have been investigated using both NADPH-diaphorase histochemistry and nNOS immunocytochemistry to label the enzyme nitric oxide synthase (NOS), and DAF-2 to label NO itself. In each case a punctate distribution of skin cells is labelled, indicating that the endogenous production of NO may regulate the properties of the skin impulse.

Key words: nitric oxide, tadpole, modulation, skin impulse.

### Introduction

The skin is the main interface between the external environment and internal body structures of an organism and as such represents a strategic point of defense. Typically, the skin is a passive structure that acts as a protective barrier, and lacks a means of direct communication between constituent cells. However, the skin of many amphibian tadpoles functions as a sensory system in its own right. For a brief period from mid-embryonic until early larval development, cells of the tadpole skin exhibit properties of nervous tissue when presented with a noxious stimulus anywhere on their surface (reviewed in Roberts, 1998). This excitability takes the form of an action potential or 'skin impulse,' which resembles a cardiac action potential in duration and waveform, and propagates from the point of initiation throughout the skin *via* electrical connections between neighbouring cells. A range of anurans, including the South African clawed frog *Xenopus laevis* (Daudin), the common frog *Rana temporaria*, the common toad *Bufo bufo*, and salamanders such as *Amystoma*, have been shown to display such excitability (Roberts, 1998). One known function of the skin impulse is to trigger escape behaviour and thereby allow the tadpole to evade predation.

In *Xenopus*, the skin impulse pathway is one of two sensory systems in the skin that operate in parallel (Roberts and Smyth, 1974), the second one involving a more conventional innervation by mechanosensory Rohon-Beard (R-B) cells, a subset of extra-ganglionic sensory neurones (Hughes, 1957). In early embryos, at stage 27 [about 24 h post-fertilization

(Nieuwkoop and Faber, 1956)], the skin is already excitable, including in areas yet to be innervated by R-B cells. Both the skin impulse and the R-B cells can activate neural circuitry of the spinal cord to initiate trunk flexion in young embryos and rhythmic swimming movements in older embryos and larvae, but through different routes. R-B cells directly activate spinal neurons (Clarke et al., 1984; Sillar and Roberts, 1988), while the skin impulse appears to gain access to the central nervous system (CNS) *via* a branch of the trigeminal nerve, bypassing primary sensory R-B neurons in the skin (Roberts, 1996). Thus the electrically excitable epithelium functions as a *bona fide* sensory system, which initially precedes and then operates in parallel with more conventional mechanosensory innervation, before its excitable properties disappear during later larval life.

Most cutaneous sensory systems are subject to modification under different circumstances (Sillar, 1989). The presence of a range of neuromodulatory substances in the skin of *Xenopus* raises the possibility that the skin impulse and its propagation through the epithelium may be subject to regulation, as is the case for other, more conventional sensory systems. One such modulator, which is produced by the skin of many vertebrates, including humans (Weller, 1997), is the free radical, nitric oxide (NO). NADPH-diaphorase labeling, a marker for the presence of the NO synthetic enzyme NOS, has been noted in some cells of the skin of *Xenopus* embryos at the hatchling stage (37/38), suggesting NO production in the epidermis (McLean and Sillar, 2000; McLean et al., 2001) and a possible role in modulating the skin impulse. Similar labeling is also found in the skin at

equivalent stages of development in *Rana* (McLean et al., 2001).

In the present paper we have investigated the modulatory effects of NO on the duration and rate of propagation of the skin impulse in hatchling *Xenopus* tadpoles and report a profound effect on both parameters. The NO donor, SNAP, reduces the rate of propagation and increases the duration of the impulse, an effect that is countered by the NO scavenger C-PTIO. SNAP also produces a significant depolarization of the membrane potential of skin cells. The endogenous source of NO has been explored using a range of anatomical techniques, revealing a scattered distribution of NO-producing skin cells over the entire surface of the tadpole. This raises the possibility that the endogenous release of NO modulates the properties of the skin impulse, and the circumstances under which this might occur are discussed.

## Materials and methods

### Animals

*Xenopus laevis* (Daudin) embryos at the stage of hatching (Nieuwkoop and Faber, 1956) were obtained by induced breeding of pairs of adults selected from a laboratory colony. Eggs were collected and reared in aerated trays at temperatures of approximately 17–23°C to stagger their development until they had reached the desired stage.

### Electrophysiology

For extracellular recordings of the skin impulse and/or ventral root activity, animals were first immobilized in 12.5  $\mu\text{mol l}^{-1}$   $\alpha$ -bungarotoxin (Sigma, Gillingham, Dorset, UK), before being transferred to a recording bath filled with recirculating Hepes-buffered saline (composition in  $\text{mmol l}^{-1}$ : 115 NaCl, 2.5 KCl, 2.5  $\text{NaHCO}_3$ , 10 Hepes, 1  $\text{MgCl}_2$  and 2  $\text{CaCl}_2$ , adjusted to pH 7.4 with NaOH). Saline was gravity-fed from a 100 ml reservoir into a Perspex<sup>TM</sup> chamber (c. 5 ml volume) containing a platform with a Sylgard<sup>TM</sup> (Dow-Corning, Midland, MI, USA) surface onto which the immobilized animals were secured with fine etched tungsten pins through the notocord. In some experiments an area of skin on the left side of the flank was removed using fine etched tungsten needle to allow a ventral root recording to be made by positioning an extracellular glass suction electrode over an intermyotomal cleft (Fig. 1A). Initiation of the skin impulse and fictive swimming was accomplished by stimulating through a second glass suction electrode, placed on the tail skin, which delivered a 1 ms current pulse *via* a DS2A isolated stimulator (Digitimer, Welwyn Garden City, UK). Signals were amplified using differential AC amplifiers (A-M Systems Model 1700, Carlsborg, WA, USA), displayed on a digital oscilloscope, digitized using a CED micro 1401 and stored and processed on a PC computer using Spike2 software (Cambridge Electronic Design v. 3.21).

For intracellular recordings of skin cells, sharp microelectrodes were pulled from filamented borosilicate glass (1.0 mm o.d., 0.58 mm i.d.; Harvard Apparatus, Ltd, Holliston, MA, USA) using a P-2000 laser puller (Sutter Instruments Co., Novato, CA, USA). Electrodes were filled with 3  $\text{mol l}^{-1}$  KCl and had resistances of 100–300 M $\Omega$ . Signals were amplified with a custom-built DC amplifier

(courtesy of Dr Steve Soffe, University of Bristol, UK). Penetration of skin cells was achieved by a brief capacity overcompensation, normally revealing a resting potential of approx. –50 to –80 mV. Cells were recorded for as long as the penetration could be maintained, but in most cases recordings were stable for only a few minutes. With unrecoverable cell loss, the electrode was withdrawn to above the surface of the epidermis, moved a few tens of  $\mu\text{m}$  laterally, and then lowered again to record from another skin cell. The sharp electrode technique allowed serial recordings of multiple skin cells to be sampled before, during and after drug applications. In addition, experiments were performed using the whole-cell patch clamp technique, which allowed stable, long-term recordings of the skin impulse; the data obtained using either technique were very similar (Fig. 1B,C). For patching of skin cells, an area of the outer layer of the two-cell thick epithelium, usually over the yolk sac (Fig. 1A; ‘YS’), was carefully peeled away using fine-etched tungsten needles and watchmaker’s forceps. Patch electrodes (ca. 10 M $\Omega$ ) were pulled on a Narishige puller (model PP-830, Willow Way, London, UK) and filled with intracellular solution (in  $\text{mmol l}^{-1}$ : 100 potassium gluconate, 2  $\text{MgCl}_2$ , 10 EGTA, 10 Hepes, 3  $\text{Na}_2\text{ATP}$ , 0.5 Na-GTP, adjusted to pH 7.3 with KOH). Recordings in whole-cell mode were amplified with an Axoclamp 2B amplifier and displayed on a PC using Spike 2 software. All reagents were obtained from Sigma or Tocris Bioscience (Bristol, Avon, UK). SNAP was also provided by the School of Chemistry, University of St Andrews, Scotland.

Electrophysiological data were analysed using Dataview software (v 4.7c, courtesy of Dr W. J. Heitler). Extracellular recordings were used to measure both motor bursts from the ventral root of the spinal cord during fictive swimming, and the voltage associated with the skin impulse from a population of epidermal cells. In some experiments, the swimming cycle period and episode duration were measured as a positive control to confirm that applied drugs (e.g. SNAP) produced effects on these parameters similar to those previously documented (McLean and Sillar, 2000). The duration of the intracellular skin impulse was measured as the interval between the initial rapid depolarization to the point where the membrane potential returned to rest. Skin impulse delay was calculated as the interval between the stimulus artefact and the onset of the rising phase of the impulse. All raw data consisting of measurements from multiple skin cells were imported into Excel spreadsheets, where data from each period (i.e. control, drug and wash) were averaged for duration and membrane potential. To analyze changes in delay, data from the entire periods before, during and after drug application were fitted to linear regression lines, and the slopes of these lines were compared using a one-way ANOVA. This method was chosen because drug-induced changes in delay were gradual, and because in some experiments they continued for a period during the subsequent wash phase, thus contaminating the average of that phase of the experiment. Measuring the slope of the phase reduced this confounding effect. Sharp microelectrode measurements during an experiment were subject to a skin cell being penetrated, and were thus made at irregular intervals, but allowed sampling of multiple cells during each experiment. In contrast, patch

microelectrode recordings were usually maintained for the duration of an experiment, and thus yielded continuous data, albeit from only one cell per preparation. ANOVAs were performed on sharp electrode data to determine if there was a statistically significant difference between periods of a given experiment. These data were pooled from multiple skin cells from each period and averaged; either the average value for duration and membrane potential, or the average slope for delay. Tukey's *post-hoc* test was used to determine statistical significance between control, drug and wash periods.

#### Anatomy

The general topography of the skin surface was studied by immersing stage 37/38 wild-type embryos in a dilute mixture of two vital dyes, Methylene Blue and Fast Green in tapwater, for 5–10 min. This procedure enhanced visualization of the boundaries between skin cells. Animals were removed from the solution, immobilized in MS222 and the flank skin was peeled off, mounted on a slide in HEPES-buffered saline and topped with a coverslip, ready for viewing.

#### NADPH-d histochemistry

The NADPH diaphorase (NADPH-d) histochemical method was applied as described previously (McLean and Sillar, 2000) but to whole embryos and excised skin patches from stage 37/38 *Xenopus*. Both wild-type and albino embryos (the latter were used to enhance contrast) were fixed in 4% paraformaldehyde (pH 7.4, 4°C) for 2 h on a rocking agitator. The animals were then washed in phosphate buffer (PB; 3×5 min), transferred to 30% sucrose in 0.1 mol l<sup>-1</sup> PB and stored in the refrigerator until they sank. Animals were then immersed in 5 ml of NADPH-d staining solution [consisting of 5 mg NADPH (Sigma N-1630), 4.95 ml 0.3% PB-TX, and 50 µl Nitroblue Tetrazolium salt (NBT; Sigma N-6639) made up from 5 mg NBT dissolved in 0.5 ml PB-TX] and incubated at 37°C for 2 h. Animals were then washed in 0.1 mol l<sup>-1</sup> PB (3×5 min), dehydrated in acetone/alcohol series and cleared in xylene before being mounted with DPX in a cavity slide, sealed and topped with a coverslip, ready for viewing.

#### nNOS immunofluorescence

Neuronal NOS (nNOS) immunocytochemistry was performed using protocols developed previously for *Xenopus* (Ramanathan et al., 2006). Animals were fixed in 4% paraformaldehyde (pH 7.4) for 2 h at room temperature on a rocker (Grant-Bio PMR-30, Shepreth, Cambridgeshire, UK), washed in 0.1 mol l<sup>-1</sup> PB (3×5 min), then placed in 5 ml of blocking serum and primary antibody. This solution consisted of 5% normal goat serum (Jackson Immuno: 005-000-121, Westgrove, PA, USA); 3% bovine serum albumin in PBS-TX (pH 7.4; 0.9% PBS plus 0.3% Triton X-100); and primary rabbit polyclonal antibody [1:100 v/v, NOS-1 (R-20):sc-648, Santa Cruz Biotechnology, Inc., Santa Cruz, CA, USA]. Following incubation at 37°C for 24 h, samples were washed in 0.1 mol l<sup>-1</sup> PBS (3×10 min), then incubated in the dark in diluent and secondary antibody (pH 7.4; AffiniPure Goat Anti-Rabbit IgG, Jackson Immuno) at 1:100 v/v for 24 h. Samples were then washed in 0.9% PBS for 24 h, mounted with Citifluor and topped with a coverslip, as above.

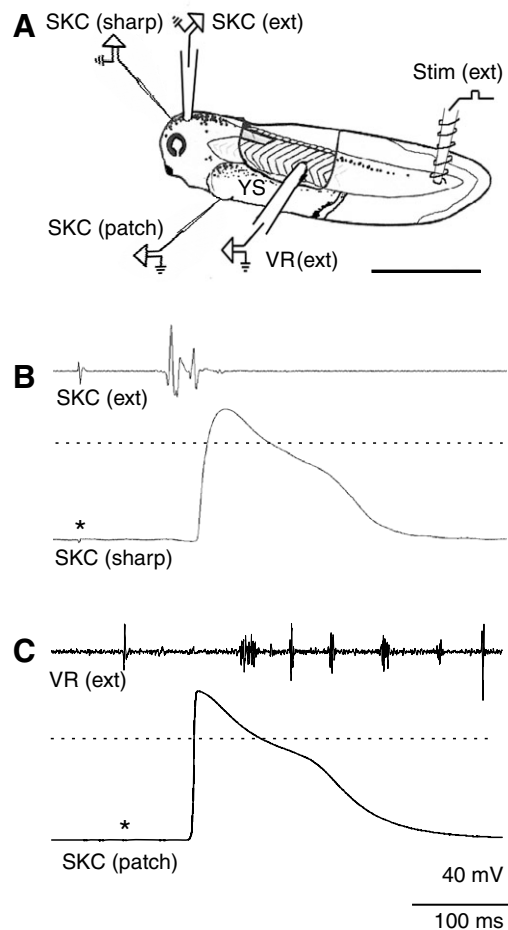


Fig. 1. (A) Schematic diagram of the preparation used to initiate and monitor skin impulses in stage 37/38 *Xenopus* embryos. SKC (sharp), sharp microelectrode for intracellular recording from skin cells; SKC (patch), patch microelectrode for intracellular recording from skin cells; SKC (ext), extracellular recording suction electrode on skin; Stim (ext), extracellular stimulating suction electrode on skin; VR (ext), extracellular recording suction electrode on ventral root; YS, yolk sac. Scale bar, 1 mm. (B) Intracellular recording from a skin cell with a sharp microelectrode (lower trace) reveals a long duration impulse that is approximately coincident with a multi-phasic impulse recorded extracellularly from a nearby patch of skin (upper trace). (C) Intracellular recording with a patch microelectrode (lower trace) reveals a skin impulse with a similar shape to that recorded with a sharp microelectrode, except that the rising phase is faster. The same stimulus that initiates a skin impulse initiates swimming monitored by an extracellular recording from the ventral root (upper trace). (B,C) The broken horizontal line is set at 0 mV. The asterisk indicates the time of the stimulus.

#### DAF-2 DA fluorescent labelling

Animals were immersed in a solution of 1 µl ml<sup>-1</sup> DAF-2 DA (4,5-diaminofluorescein diacetate; Calbiochem, La Jolla, CA, USA) in HEPES saline, then placed on a rocking agitator for 15–30 min. The staining solution was replaced with 4% paraformaldehyde in PB (pH 7.4, 4°C) for 2 h. After fixation, animals were washed in 0.1 mol l<sup>-1</sup> PB (3×5 min), mounted in a glass cavity slide, using Citifluor (glycerol solution, AF2), then coverslips placed on top. The edges of the coverslips were affixed using clear nail varnish. In some experiments tadpoles

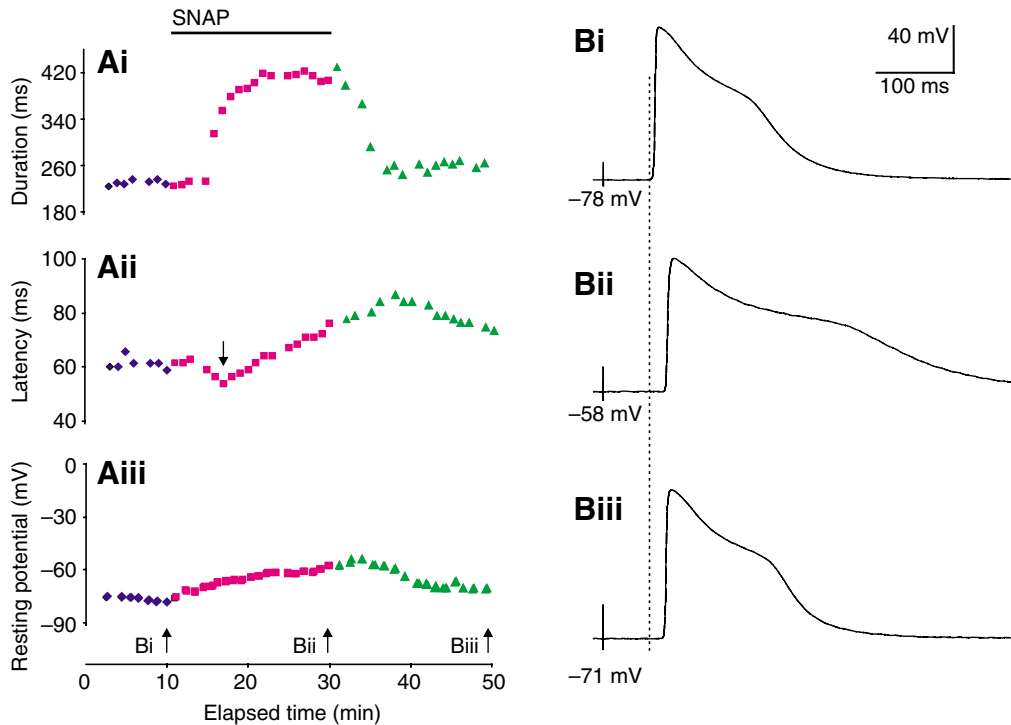


Fig. 2. The effects of the NO donor SNAP on skin cell electrophysiology. (A) Sequential measurements from a patch recording of a single skin cell, which was maintained throughout the experiment. SNAP (horizontal line) reversibly increases the impulse duration (Ai) and the delay from stimulus (Aii, but note that there is an initial decrease in delay; down arrow) and decreases the resting membrane potential (Aiii). Control (pre-application) data are shown as blue diamonds, SNAP data are magenta squares, and wash data are green triangles. (B) Individual responses to stimuli applied at times indicated by the up arrows above the time axis in (A). The resting membrane potential is shown at the start of each record. The records are aligned at the time of the stimulus, and the vertical broken line indicates the response delay in control conditions. Times to peak of skin impulses were 11.3 ms in control (Bi), 13.6 ms in SNAP (Bii) and 12.6 ms in wash (Biii).

were anaesthetized in MS222 then mounted in the staining solution, placed beneath a coverslip and viewed using an epifluorescence microscope. This method revealed that the optimum time for DAF-2DA labeling was 15–30 min; after more than approximately 2 h the fluorescence of skin cells all but disappeared.

Images of Methylene Blue/Fast Green-treated preparations and NADPH-d labeling were obtained using a Zeiss Axiolab microscope coupled to a Sony digital camera. nNOS immunolabeling and DAF2-DA images were obtained on either a Leica multiphoton confocal microscope or a Nikon Eclipse T5100 fluorescence microscope.

## Results

### *Basic properties of the skin impulse*

The basic properties of the skin impulse (Fig. 1) were found to be similar to those reported previously (Roberts, 1971; Roberts and Stirling, 1971). The skin impulse was triggered by a stimulus applied to the caudal tail [Fig. 1A, Stim (ext)] and recorded either intracellularly on the head region with sharp electrodes [Fig. 1A, SKC (sharp); Fig. 1B, bottom trace] or on the flank using patch electrodes [Fig. 1A, SKC (patch); C, bottom trace]. In some experiments the skin impulse and/or ventral root activity were also recorded extracellularly [Fig. 1A, SKC (ext), VR (ext); B,C top traces].

Intracellular recordings with either sharp or patch electrodes reveal an overshooting skin impulse with a characteristic

waveform that superficially resembles a cardiac action potential (Fig. 1B,C). The only obvious difference between the two recording techniques is that the patch recordings have a sharper rising phase (time to peak ca. 5 vs 30 ms), presumably due to the lower electrode capacitance. There is a relatively rapid rising phase, which is followed by a longer plateau phase (ca. 60 ms to 150 ms) and then by a slow decay back to rest. The total duration of the impulse varied with different recordings, but under control conditions was usually in the range of 150 to 200 ms. The onset of the rising phase of the skin impulse had a delay from the stimulus of 60 to 100 ms (Fig. 1B,C) which, with a separation between stimulating and recording electrodes of approximately 4 mm (Fig. 1A), equates to a conduction velocity of approximately 4–7 cm s<sup>-1</sup>, similar to that reported previously [5–11 cm s<sup>-1</sup> (Roberts, 1971)]. The measured conduction delay varied within and between different preparations and depended upon a range of parameters including stimulus frequency, with higher frequencies increasing delay (not illustrated). The extracellular recordings showed a complex, multi-phasic waveform presumably reflecting the relatively rapid rising phases of several skin cells located beneath the recording electrode. The subsequent slower phases of the impulses were attenuated due to the high-pass filter characteristics of the extracellular amplifier. A supra-threshold stimulus that initiated a skin impulse usually also initiated an episode of fictive swimming, as recorded using a suction electrode positioned over a ventral root (Fig. 1C, top trace).

*The effects of the NO donor, SNAP*

The NO donor, SNAP [200–500  $\mu\text{mol l}^{-1}$  (see also McLean and Sillar, 2000)] was bath-applied to investigate the potential modulatory effects of NO on the skin impulse. SNAP had three consistent and highly significant ( $P < 0.01$ ) effects (Figs 2, 3): (1) it increased the duration of the skin impulse (Fig. 2Ai,Bii, Fig. 3A); (2) it increased the delay from the stimulus to the skin impulse (Fig. 2Aii,B, Fig. 3B); and (3) it caused the membrane potential to depolarize (Fig. 2Aiii,B, Fig. 3C). These effects were apparent in both patch (Fig. 2;  $N=5$ ) and sharp-electrode (Fig. 3;  $N=27$ ) recordings. The increase in duration became clear shortly after the application of SNAP, and its rise to a stable maximum was relatively rapid (e.g. Fig. 2Ai). The duration increase reversed significantly towards baseline levels with wash (Fig. 3A;  $P < 0.05$ ). In contrast, the delay consistently showed a brief but significant ( $P < 0.05$ ) decrease immediately following SNAP application (down arrow in Fig. 2Aii), followed by a slow increase. This increase frequently continued even in the initial stages of the wash, although it usually started to gradually reverse with sustained washing (Fig. 2Aii). The delay did not usually completely return to baseline within the time period of an experiment, although the reversal was significant ( $P < 0.05$ ). Similarly, the effect on membrane potential was gradual in onset and only partially reversed on washout (Fig. 2Aiii, Fig. 3C). To control for vehicle-related effects, 0.5% dimethyl sulfoxide (DMSO) was applied on its own. In pooled data for six cells, no significant changes were observed for delay, duration or resting potential (not illustrated). In summary, the delay and duration of the skin impulse and the resting potential of skin cells are significantly affected by SNAP; these effects are not vehicle related and therefore are presumably mediated by NO.

*The effects of the NO scavenger, C-PTIO*

The NO scavenger, C-PTIO (500  $\mu\text{mol l}^{-1}$ ), was added in the presence of SNAP (Fig. 4;  $N=9$ ), to support the proposal that these effects of SNAP are indeed due to the exogenous elevation of NO. The average skin impulse duration showed a significant increase in the presence of SNAP (Fig. 4Ai,Bi;  $P < 0.01$ ), and this effect was significantly reversed by adding C-PTIO. Skin impulse delay doubled from approximately 60 ms to 120 ms within 25 min of the application of SNAP (Fig. 4Aii), then decreased markedly shortly after C-PTIO was added (Fig. 4Aii,Bii). The SNAP-induced depolarization of skin cells was also significantly counteracted by C-PTIO (Fig. 4Aiii). In pooled data (Fig. 4Biii;  $N=9$ ) the SNAP effect was significantly ( $P < 0.05$ ) reversed, with the membrane potential returning close to control levels in C-PTIO. In summary, all three of the SNAP-induced changes in skin cells are reversed when NO is scavenged by C-PTIO, suggesting that the effects are most likely due to the release of exogenous NO.

*The endogenous source of NO in the skin*

The preceding pharmacological experiments using the NO donor, SNAP, and the scavenger, C-PTIO, raise the possibility that NO released from an endogenous source could modulate the excitability of the skin and the propagation of the skin impulse. At the hatching stage the skin surface comprises an array of 5- or 6-sided cells of approximately 20  $\mu\text{m}$  diameter

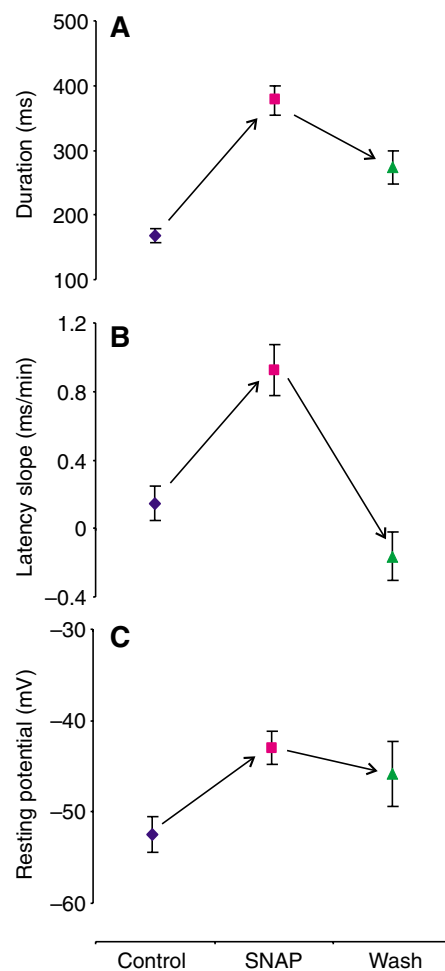


Fig. 3. (A) Pooled data from 27 preparations showing SNAP effects on skin cell impulse duration (A) and delay from stimulus (B) and skin cell resting potential (C). In each preparation measurements of each parameter were taken with sharp microelectrodes from at least 8 different skin cells in control (blue diamond), SNAP (magenta square) and wash (green triangle) conditions. Single representative values for each parameter in each condition were obtained from each preparation as the average of the duration and resting potential measurements, and the least-squares regression slope of the delay measurements. Values are means  $\pm$  s.e.m. of these representative values.

(Fig. 5A). A previous study using the NADPH-d technique provided preliminary evidence for NOS expression in skin cells of both *Xenopus* (McLean and Sillar, 2000) and *Rana* (McLean et al., 2001). To confirm this finding, skin samples from both wild-type (Fig. 5B) and albino (Fig. 5C) stage 37/38 *Xenopus* embryos were stained using the NADPH-d technique. In both wild-type ( $N=6$ ) and albino embryos ( $N=9$ ), a proportion of skin cells, approximately one in five, displayed positive staining and although the intensity of labeling was rather variable, this punctate pattern was observed over the entire surface of the body.

Although the NADPH-d technique is a reliable marker for NOS in older stage *Xenopus* tadpole CNS neurons (Ramanathan et al., 2006), we performed NOS immunocytochemistry to confirm this with skin of hatching stage *Xenopus* embryos. Since the skin and the nervous system share a common

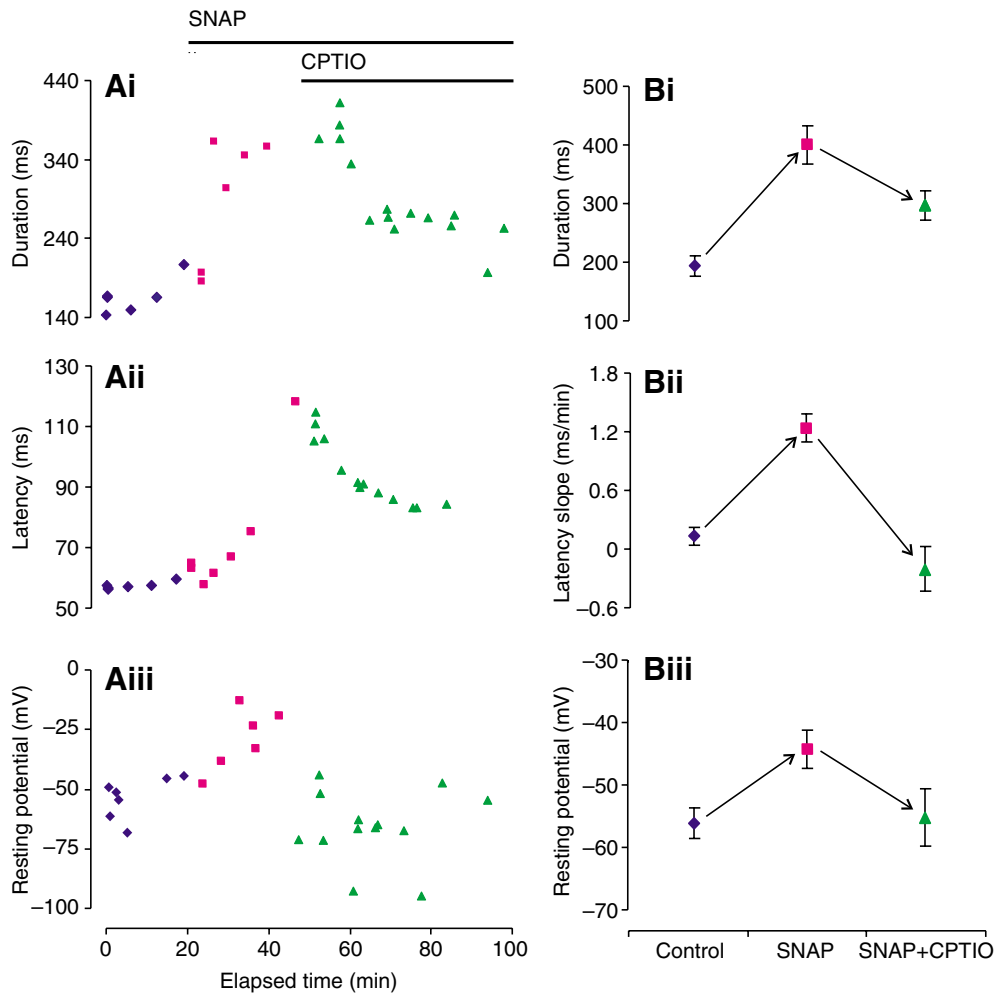


Fig. 4. CPTIO reverses the effects on SNAP. (A) Data from a single preparation in which measurements of skin impulse duration (Ai) and delay from stimulus (Aii) and skin cell resting potential (Aiii) were taken with sharp microelectrodes from different skin cells in control (blue diamond), SNAP (magenta square) and SNAP+CPTIO (green triangle) conditions. (B) Pooled data from nine preparations, with analysis similar to that of Fig. 3.

embryological origin, an nNOS antibody was used on excised pieces of skin from three stage 37/38 embryos ( $N=3$ ; Fig. 5D). nNOS-positive labeling displayed an irregular patterning in all skin patches with a distribution that was very similar to that found using the NADPH-d technique. In control preparations, where the primary antibody was omitted from the incubation schedule, no fluorescence was observed (Fig. 5E;  $N=3$ ). This suggests that the staining observed in the skin cells is specific to nNOS.

The experiments using NADPH-d and nNOS immunohistochemistry strongly suggest that a sub-population of skin cells possess the enzyme necessary for generating NO. To investigate further whether NO is actually produced by cells in the skin, as has been shown at later premetamorphic stages (Wilding and Kerschbaum, 2007), stage 37/38 *Xenopus* embryos were treated with the fluorescent probe DAF-2 DA, a cell-permeable molecule converted into the cell-impermeable DAF-2 by intracellular esterases. Within NO-generating cells, NO binds DAF-2 to form fluorescent triazolofluorescein. Green fluorescence, indicating the presence of NO, was found in about

20% of cells, dispersed over the entire surface of the animal in whole-mount preparations (Fig. 5F;  $N=12$ ). This punctate pattern of staining in the skin was observed over the entire surface of the body, although the clearest fluorescent signal was found in the fin of the tadpole, where only skin cells are present. Thus, the appearance of DAF fluorescence in the skin suggests that skin cells are not only NOS positive, but actually produce NO from these early stages of development.

### Discussion

In this investigation, we have provided new evidence that NO may be an endogenous modulator of the skin cell sensory pathway. We have shown that exogenous NO changes the duration and conduction delay of the skin impulse and the resting membrane potential of skin cells. We have also shown that a sub-population of skin cells with a punctate distribution are an endogenous source of NO, confirming and extending observations made in previous studies (McLean and Sillar, 2001; Wilding and Kerschbaum, 2007). NO-producing cells are distributed apparently randomly and scattered throughout the

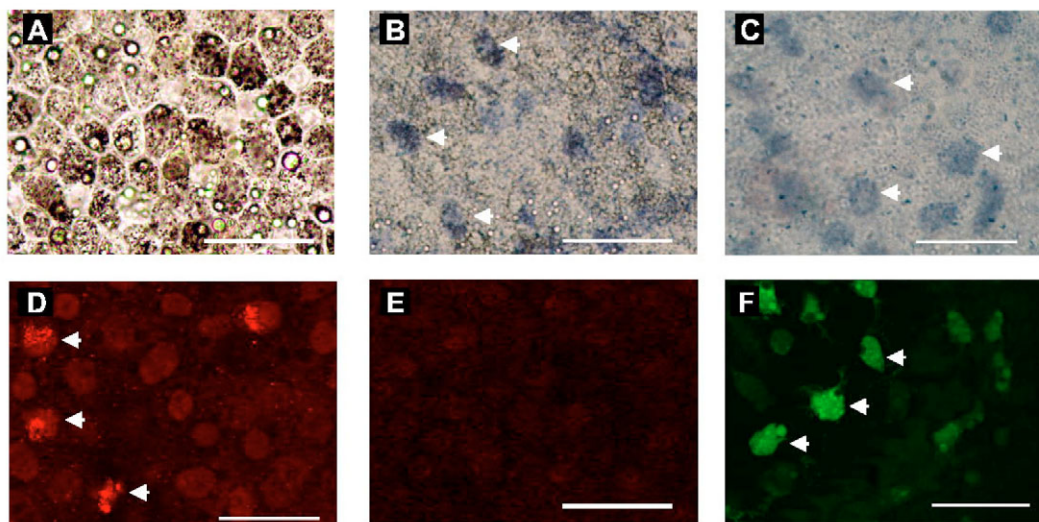


Fig. 5. Location of NOS and NO production in *Xenopus* embryo skin. (A) Bright-field image of skin surface of wild-type embryo showing general topography of skin cells, some of which are pigmented. Small white spheres are yolk platelets. (B) Punctate pattern of NADPH-diaphorase labelling in wild-type skin cells (blue label). Note diffuse background pigmentation (darker, grey). (C) Similar pattern of NADPH-diaphorase labelling in skin of albino embryo, which lacks pigmentation. (D) nNOS immunofluorescence labels a similar proportion of skin cells. (E) Example of control nNOS experiment in which the primary antibody was omitted and no labeled cells were detectable. (F) DAF2 marks cells producing NO, with similar distribution in skin. White arrows indicate examples of strongly labeled cells (in B, C, D and F). Scale bars, 50  $\mu\text{m}$ . See text and Materials and methods for further details.

skin of hatchling *Xenopus* tadpoles. Given this spatial organization of NOS, global upregulation of NO produced in the skin may modulate the skin sensory pathway over the entire body surface, or local increases in NOS activity could occur in response to a focal challenge, producing a spatially restricted response. However, the circumstances responsible for triggering NO release have not been investigated.

#### *Modulation of the skin impulse by NO*

Several neuroactive substances produced in the skin of amphibians, including NO (McLean and Sillar, 2001; Wilding and Herschbaum, 2007; Zaccone et al., 2006), biogenic amines and peptides (Erspamer, 1971), could in principle modulate the skin impulse, either by acting on the biophysical properties of individual skin cells, or on the propagation of the impulse *via* direct gap junctional coupling between cells, or both. In this paper we have addressed the possibility that NO functions in this capacity. Experiments with the NO donor, SNAP, have led to three new findings: (1) SNAP produces a fast, large and reversible increase in the duration of the skin impulse; (2) SNAP reversibly decreases the conduction velocity of the skin impulse as it propagates across the epithelium; and (3) SNAP depolarizes skin cells. The effects of SNAP on each of these parameters can be reversed by the NO scavenger, C-PTIO.

The skin impulse comprises a fast rising phase that is thought to be  $\text{Na}^+$ -dependent (Roberts, 1971), a slower plateau phase, and a relaxation phase that returns the membrane potential back to rest. The ionic bases of the plateau and relaxation phases are not known, but the increase in duration in the presence of SNAP is likely to be due to effects on these later phases, because the rise time of the impulse is not markedly affected by SNAP (Fig. 2B). The SNAP-released NO could, for example,

modulate cyclic nucleotide-gated channels (CNG) (Hofmann et al., 2005) by acting *via* a 2nd messenger such as cGMP or cAMP. Such channels could contribute to the repolarizing phase of the impulse, and/or could also underlie the SNAP-induced depolarization of skin cell resting potentials.

Given the ability of NO to uncouple gap junctions (GJs) in other systems (Fessenden and Schacht, 1998; Kameritsch et al., 2003; Kameritsch et al., 2005; Yao et al., 2005; Patel et al., 2006), the SNAP effects on delay could be explained if NO reduces the junctional coupling thought to be responsible for propagation of the impulse between the cells of the skin (Roberts, 1971). Such a reduction could increase the effective path length as the skin impulse follows a more circuitous route from the point of initiation to the recording site and/or it could reduce the rate of depolarization of successive cells in the pathway thus producing a cumulative increase in propagation delay. Connexins and their resulting intercellular GJs are present in the early embryo (reviewed in Mackie, 1970; Warner, 1985; Kandler and Katz, 1995; Levin and Mercola, 2000; Landesman et al., 2003) and could be retained through the late embryo stage. This is important because the presence of GJs beginning at stage 22 when the skin impulse is first found (Roberts, 1971), would support Roberts' theory that the impulse propagates through the skin by direct current flow *via* low-resistance junctions.

#### *NO is present in the skin*

NADPH-d histochemistry is a technique used to localize putative NOS-containing cells. The NADPH-d reactivity found in cross sections of skin (McLean and Sillar, 2001), and the further identification of labeling in whole-mount skin samples presented here, support the conclusion that NOS is localised to a sub-population of skin cells. Staining was found in both wild-

type and albino skin, with staining being much clearer in the latter due to the lack of pigment obscuring the labelling. However, NADPH specificity for NOS can be unreliable (cf. Vincent, 1995). The appearance of nNOS immunofluorescence in excised skin patches confirmed the presence of NOS in skin cells of *Xenopus* embryos at stage 37/38, with the pattern of staining being similar to the punctate distribution of NADPH-d staining. During vertebrate development, the skin is derived from the ectodermal tissue. This early germ layer also differentiates into nervous tissue. Thus, nNOS present in skin cells at stage 37/38, may be retained from synthesis at earlier stages in development. During the time of gastrulation, cells could express the NOS enzyme before diverging to become either part of the CNS where NOS is expressed in brainstem neurons at early embryonic stages (McLean and Sillar, 2001), or part of the epidermis, as indicated by the nNOS immunofluorescence reported here.

DAF-2 fluorescence was used to visualize the endogenous production of NO in skin cells and a punctate pattern of staining was again found, suggesting that NO is produced by about 20% of skin cells, similar to the distribution of NADPH-d and nNOS staining. Taken together these results suggest that NOS and NO colocalize in the same skin cells. The identification of endogenous NO through DAF-2 labelling suggests that NO is being released as an autocrine or paracrine messenger. The punctate distribution of NOS across the skin, together with the ease with which NO can diffuse through tissue, suggests that NO can affect the entire surface of the tadpole.

A similar distribution of NADPH diaphorase labeling and NO production has been described in the skin at later stages of *Xenopus* tadpole development (Wilding and Kerschbaum, 2007), where NO has been implicated in the regulation of ammonium release. In a related amphibian species, *Triturus italicus*, the endothelial isoform of NOS (eNOS) is expressed strongly in the larval skin (Brunelli et al., 2005), but this begins to disappear in pre-metamorphic and metamorphic periods coincident with a simultaneous rise in expression of the inducible isoform of NOS (iNOS). This suggests that in *Triturus*, a switch occurs in the developmental cycle, and NOS-derived NO may be responsible for the remodeling of skin cells during the metamorphic period.

#### Functional considerations

Given that NO appears to be produced and released by a proportion of skin cells and is capable of modulating skin physiology, what might be the role of this phenomenon for the hatchling tadpole? One possibility is that the NO alters the properties of the skin pathway for eliciting escape responses. The threshold stimulus to evoke the skin impulse did not appear to change during the bath application of SNAP (not illustrated), however, suggesting that NO does not normally modulate the sensitivity of this sensory pathway. The increased duration of the skin impulse might enhance the efficacy of its transmission to the central nervous system, although the behavioural advantage of slowing skin impulse propagation is unclear. Another possibility is that NO is involved in the response to tissue damage. Noxious stimuli to the skin could increase NO production, and it is known that NO can enhance repair processes (reviewed in Witte and Barbul, 2002). NO-induced

gap junction uncoupling could reduce the leakage of intracellular contents from intact cells through damaged tissue, while the increased duration of the skin impulse will prolong activation of voltage-dependent channels and could thus have profound effects on intracellular second messengers, including those potentially involved in wound healing.

We have shown that a widespread but punctate population of skin cells contain the crucial enzyme for producing NO and that a similar population do indeed have elevated levels of NO. This population could thus act as a source to trigger the significant NO effects on skin cell properties that we have documented, notably the changes in the rate of propagation and waveform of the skin impulse. Taken together, our data point to NO as a potent modulator of the skin impulse in *Xenopus laevis*.

#### List of abbreviations

CNG	cyclic nucleotide gated channel
CNS	central nervous system
C-PTIO	2-(4-carboxyphenyl)-4,4,5,5-tetramethylimidazoline-1-oxyl-3-oxide
DAF-2	diaminofluorescein-diacetate
DMSO	dimethyl sulfoxide
GJ	gap junction
NAD	nicotinamide adenine dinucleotide
NADPH-d	NADPH diaphorase
NBT	Nitroblue Tetrazolium
nNOS	neuronal nitric oxide synthase
NO	nitric oxide
NOS	NO synthase
PB	phosphate buffer
PB-TX	PB + Triton X-100
RB	Rohon-Beard neuron
SKC	skin cell
SNAP	S-nitroso-N-acetylpenicillamine
VR	ventral root
YS	yolk sac

This work was supported by a grant from the BBSRC to K.T.S. and W.J.H., to whom we are grateful.

#### References

- Brunelli, E., Perrotta, I., Talarico, E. and Tripepi, S. (2005). Localization of two nitric oxide synthase isoforms, eNOS and iNOS, in the skin of *Triturus italicus* (Amphibia, Urodela) during development. *Comp. Biochem. Physiol.* **142A**, 249-255.
- Clarke, J. D., Hayes, B. P., Hunt, S. P. and Roberts, A. (1984). Sensory physiology, anatomy and immunohistochemistry of Rohon-Beard neurones in embryos of *Xenopus laevis*. *J. Physiol.* **348**, 511-525.
- Erspamer, V. (1971). Biogenic amines and active polypeptides of amphibian skin. *Annu. Rev. Pharmacol.* **11**, 327-350.
- Fessenden, J. D. and Schacht, J. (1998). The nitric oxide/cyclic GMP pathway: a potential major regulator of cochlear physiology. *Hear. Res.* **118**, 168-176.
- Hofmann, F., Biel, M. and Kaupp, U. B. (2005). International Union of Pharmacology. LI. Nomenclature and structure-function relationships of cyclic nucleotide-regulated channels. *Pharmacol. Rev.* **57**, 455-462.
- Hughes, A. (1957). The development of the primary sensory system in *Xenopus laevis* (Daudin). *J. Anat.* **91**, 323-338.
- Kameritsch, P., Hoffmann, A. and Pohl, U. (2003). Opposing effects of nitric oxide on different connexins expressed in the vascular system. *Cell Commun. Adhes.* **10**, 305-309.
- Kameritsch, P., Khandoga, N., Nagel, W., Hundhausen, C., Lidington, D. and Pohl, U. (2005). Nitric oxide specifically reduces the permeability of

- Cx37-containing gap junctions to small molecules. *J. Cell. Physiol.* **203**, 233-242.
- Kandler, K. and Katz, L. C.** (1995). Neuronal coupling and uncoupling in the developing nervous system. *Curr. Opin. Neurobiol.* **5**, 98-105.
- Landesman, Y., Postma, F. R., Goodenough, D. A. and Paul, D. L.** (2003). Multiple connexins contribute to intercellular communication in the *Xenopus* embryo. *J. Cell Sci.* **116**, 29-38.
- Levin, M. and Mercola, M.** (2000). Expression of connexin 30 in *Xenopus* embryos and its involvement in hatching gland function. *Dev. Dyn.* **219**, 96-101.
- Mackie, G. O.** (1970). Neuroid conduction and the evolution of conducting tissues. *Q. Rev. Biol.* **45**, 319-332.
- McLean, D. L. and Sillar, K. T.** (2000). The distribution of NADPH-diaphorase labelled interneurons and the role of nitric oxide in the swimming system of *Xenopus* larvae. *J. Exp. Biol.* **203**, 705-713.
- McLean, D. L. and Sillar, K. T.** (2001). Spatiotemporal pattern of nicotinamide adenine dinucleotide phosphate-diaphorase reactivity in the central nervous system of premetamorphic *Xenopus laevis* tadpoles. *J. Comp. Neurol.* **437**, 350-362.
- McLean, D. L., McDearmid, J. R. and Sillar, K. T.** (2001). Induction of a non-rhythmic motor pattern by nitric oxide in *Rana temporaria* frog embryos. *J. Exp. Biol.* **204**, 1307-1317.
- Nieuwkoop, P. D. and Faber, J.** (1956). *Normal Tables for Xenopus laevis*. Amsterdam: North Holland.
- Patel, L. S., Mitchell, C. K., Dubinsky, W. P. and O'Brien, J.** (2006). Regulation of gap junction coupling through the neuronal connexin Cx35 by nitric oxide and cGMP. *Cell Commun. Adhes.* **13**, 41-54.
- Ramanathan, S., Combes, D., Simmers, J. and Sillar, K. T.** (2006). Developmental and regional NADPH-diaphorase labeling in spinal cord neurons of metamorphosing *Xenopus laevis*: correlation of nitric oxide synthase expression with the emergence of limb motor networks. *Eur. J. Neurosci.* **24**, 1907-1922.
- Roberts, A.** (1971). The role of propagated skin impulses in the sensory system of young tadpoles. *Z. Vergl. Physiol.* **75**, 388-401.
- Roberts, A.** (1996). Trigeminal pathway for the skin impulse to initiate swimming in hatching *Xenopus* embryos. *J. Physiol.* **493P**, 40P-41P.
- Roberts, A.** (1998). Skin sensory systems of amphibian embryos and young larvae. In *Amphibian Biology*, Vol. 3. *Sensory Perception* (ed. H. Heatwole), pp. 923-935. Chipping Norton, Australia: Surrey Beatty & Sons.
- Roberts, A. and Smyth, D.** (1974). The development of a dual touch sensory system in embryos of the amphibian *Xenopus laevis*. *J. Comp. Physiol.* **88**, 31-42.
- Roberts, A. and Stirling, C. A.** (1971). The properties and propagation of a cardiac-like impulse in the skin of young tadpoles. *Z. Vergl. Physiol.* **71**, 295-310.
- Sillar, K. T.** (1989). Synaptic modulation of cutaneous pathways in the vertebrate spinal cord. *Semin. Neurosci.* **1**, 45-54.
- Sillar, K. T. and Roberts, A.** (1988). A neuronal mechanism for sensory gating during locomotion in a vertebrate. *Nature* **331**, 262-265.
- Vincent, S. R.** (1995). Localization of nitric oxide neurons in the central nervous system. In *Nitric Oxide in the Nervous System* (ed. P. Jenner), pp. 83-102. New York, London: Academic Press.
- Warner, A. E.** (1985). The role of gap junctions in amphibian development. *J. Embryol. Exp. Morphol.* **89**, 365-380.
- Weller, R.** (1997). Nitric oxide – a newly discovered chemical transmitter in human skin. *Br. J. Dermatol.* **137**, 655-672.
- Wilding, S. and Kerschbaum, H. H.** (2007). Nitric oxide decreases ammonium release in tadpoles of the clawed frog, *Xenopus laevis*, Daudin. *J. Comp. Physiol. B* **177**, 401-411.
- Witte, M. B. and Barbul, A.** (2002). Role of nitric oxide in wound repair. *Am. J. Surg.* **183**, 406-412.
- Yao, J., Hiramatsu, N., Zhu, Y., Morioka, T., Takeda, M., Oite, T. and Kitamura, M.** (2005). Nitric oxide-mediated regulation of connexin43 expression and gap junctional intercellular communication in mesangial cells. *J. Am. Soc. Nephrol.* **16**, 58-67.
- Zaccone, G., Mauceri, A., Maisano, M. and Fasulo, S.** (2006). Immunolocalization of nitric oxide synthase in the epidermis of the tiger salamander, *Ambystoma tigrinum*. *Acta Histochem.* **108**, 407-410.